JOM, Vol. 76, No. 3, 2024
https://doi.org/10.1007/s11837-023-06295-3

Preparation of Spherical Porous and Spherical Ti6Al4V Powder by Copper-Assisted Spheroidization Method

JIN QIAN,[1] LI ZHANG,[1] and SHAOLONG TANG[1,2]

1.—Jiangsu Key Laboratory for Nanotechnology, Collaborative Innovation Center of Advanced Microstructures, National Laboratory of Solid State Microstructures, Department of Physics, Nanjing University, Nanjing 210093, People's Republic of China. 2.—e-mail: tangsl@nju.edu.cn

The properties of impurity content, particle size distribution, and sphericity of the spherical Ti6Al4V powder are very important in the field of additive manufacturing. Currently, there are some shortcomings in the common method of preparing high-quality Ti6Al4V alloy spherical powders. A copper-assisted spheroidization method for preparation of spherical Ti6Al4V powder was developed in this study. The process involved induction melting to prepare a high brittleness intermetallic Cu-Ti-Al-V pre-alloy with low melting point. The solid-liquid interface dewetting method was then used to obtain the spherical Cu-Ti-Al-V particles, which were further processed using dealloying to obtain spherical porous Ti6Al4V powder. Finally, the spherical Ti6Al4V powder was obtained by undergoing combined sintering and deoxidizing steps. The study investigated the morphologies, structure, and composition of the preparation processes. The spherical Ti6Al4V powder prepared by this method possesses controllable composition and particle size distribution, along with low oxygen content, potentially meeting the requirements of additive manufacturing.

INTRODUCTION

Titanium alloy is a non-ferrous alloy composed of the basic element Ti and other elements such as V, Al, Fe, Cu, etc.[1] Due to its low density, high heat resistance, strong fatigue resistance, and good biocompatibility, titanium alloy is widely used in various industries, including aerospace, automotive, biomedical, and marine equipment.[2,3] Among them, the Ti6Al4V (mass ratio) dual-phase titanium alloy with a typical structure of the main α-phase (HCP structure) and a small amount of β-phase (BCC structure) has the largest proportion of usage, which is close to 50%.[2,4] Despite its desirable properties, the Ti6Al4V alloy is limited in its application due to its large deformation resistance and the disadvantages of a long preparation process, complicated processing technology, and difficulty in machining precision parts. These factors contribute to the high cost and price of the alloy.[5,6]

(Received July 10, 2023; accepted November 13, 2023; published online November 29, 2023)

Additive manufacturing (AM) technology is a near net shape technology developed since the 1970s. Unlike traditional processing technologies, such as cutting and assembling raw materials, AM is a 'layer-by-layer' process that can achieve digital moldless forming manufacturing of components. This process has several advantages, including high repeatability, short production cycles, and extremely high machining accuracy. As a result, parts with complex structures can be easily manufactured, expanding the application range of titanium alloy materials.[7,8] Currently, the mostly selected Ti-6Al-4V AM technology is laser powder bed fusion (L-PBF), which adopts the spherical Ti-6Al-4V powder as the processing raw materials.[9–13] The performance of the as-built components is greatly influenced by the impurity content, particle size distribution, and sphericity of the spherical Ti-6Al-4V powder.[6] Therefore, the development of low-cost and high-quality spherical Ti-6Al-4V powder has become a research hotspot in the AM field.[14–17] Besides, at present, the main methods for preparing spherical Ti-6Al-4V powder are atomization methods like gas atomization method (GA), plasma

atomization method (PA), plasma rotating electrode method (PREP), etc.[18] When preparing the spherical powder, due to the inevitable process of air flow impacting the molten metal droplets during the GA and PA method, the products will contain hollow powder, satellite balls and other problems, which will seriously damage the performance of the final components.[18–21] The PREP method can prepare spherical powder with a narrow particle size distribution, low oxygen content, and good sphericity by adjusting the electrode speed, blank diameter, and other processes, which greatly reduces the occurrence of hollow powder and satellite balls. However, due to the high cost and low yield of fine powder, which is limited by the rotation speed of the electrode, its application is currently restricted.[22,23]

Currently, various methods have been developed for preparing spherical metal powders.[16,24] Among them, the solid-liquid interface dewetting spheroidization method is representative.[24] This method omits the atomization process and allows for adjustment of particle size, atmosphere, temperature, and holding time during the spheroidizing process to prepare the desired spherical powder specifications. It has potential to be a universal method for mass production of micron spherical metal particles.[24–26] However, this method is not suitable for high-melting titanium alloys with a high temperature affinity for oxygen.

In this work, a copper-assisted spheroidization method was proposed. First, we introduced copper element to prepare intermetallic Cu-Ti-Al-V pre-alloy by induction melting. As an intermetallic compound, the Cu-Ti-Al-V pre-alloy has a low melting point and high brittleness compared with Ti6Al4V alloy. Then, the Cu-Ti-Al-V pre-alloyed spheres were prepared by solid-liquid interface dewetting spheroidization method. Afterwards, the spherical porous Ti6Al4V powder was obtained by dealloying method. Finally, the compact spherical Ti6Al4V powder with low oxygen content was prepared through the processes of sintering and deoxidizing.

EXPERIMENTAL SECTION

The preparation processes are schematically illustrated in Fig. 1. Ingot with a mass ratio of Cu40Ti2.7Al1.8V was prepared by induction melting Cu (99.999%), Ti (99.9%), Al (99.9%), and V (99.8%) particles. The Cu40Ti2.7Al1.8V pre-alloy was ground by hand, and the irregular particles ($< 100\ \mu$m) were obtained by sieving with a 150-mesh sieve. The Cu40Ti2.7Al1.8V and Y_2O_3 particles (99.99%, 1–2 μm) were mixed uniformly in a mass ratio of 1:3, followed by putting them into a tube furnace and filling with Ar. Then, they were annealed at 1250°C for 30 min followed by cooling to room temperature with the furnace. The obtained mixed powder was ultrasonically cleaned to remove most of the Y_2O_3 particles and leached in 1 M HNO_3 for 3 h, followed by water-washing and drying in air to acquire spherical Cu40Ti2.7Al1.8V pre-alloy powder. The prepared spherical Cu40Ti2.7Al1.8V pre-alloy powders, anhydrous magnesium chloride ($MgCl_2$) powders, and atomized spherical Mg powders with a mass ratio of 2:5:5 were uniformly mixed into a molybdenum crucible. The samples were put into a tube furnace and annealed at 845°C for 30 min with flowing Ar to carry out the dealloying process. When cooled to room temperature in the furnace, the spherical porous Ti6Al4V alloy was obtained by water-washing, leaching in 3 M HNO_3 for 3 h, water-washing, and drying in air.

The Y_2O_3 particles and spherical porous Ti6Al4V alloy powder were uniformly mixed with a mass ratio of 1:3 and then put into a furnace, followed by annealing at 1200°C in an Ar atmosphere for 4 h for the sintering treatment. After sintering, the dense spherical Ti6Al4V powder was obtained by leaching, washing, and drying in air. Spherical Ti6Al4V powder, Ca particles, and KCl-$CaCl_2$ eutectic salt were uniformly mixed with a mass ratio of 1:1:1 and kept at 750°C for 20 h in an Ar atmosphere to carry out the deoxidizing process. Finally, the mixture was leached in dilute hydrochloric acid and water-washed followed by drying in air to acquire the deoxidized spherical Ti6Al4V powder.

Morphologies of the powder, cross section, and element distribution of the powder were observed by a scanning electron microscope (SEM Gemini 500) combined with energy-dispersive spectroscopy (EDS). Phase compositions of all the powders were investigated via an X-ray diffractometer (XRD) with Cu Kα radiation at 30 kV and 20 mA. The oxygen content of the powder was measured by LECO ONH836, and the particle size distribution of the final spherical Ti6Al4V powder was analyzed by LS 13 320 Particle Size Analyzer. The concentrations of metallic elements were analyzed using an inductively coupled plasma atomic emission spectrometer (ICP-AES).

RESULTS AND DISCUSSIONS

Preparation of Spherical Cu40Ti2.7Al1.8V Intermetallic Powder

Generally, as shown in Fig. 1 and Eq. 1, Young's equation is used to describe the contact angle (θ) when conducting the solid–liquid interface dewetting spheroidization method:

$$\cos\theta = \frac{\gamma_{sv} - \gamma_{sl}}{\gamma_{lv}} \quad (1)$$

where the γ_{sl}, γ_{sv}, and γ_{lv} represent the free energies of the solid/liquid, solid/vapor, and liquid/vapor interfaces, respectively. In the solid-liquid interface dewetting spheroidization method, a greater contact angle (θ) indicates a lower wettability between the metal droplets and solid dispersant powder. As a result, the shrinking metal droplets in a molten

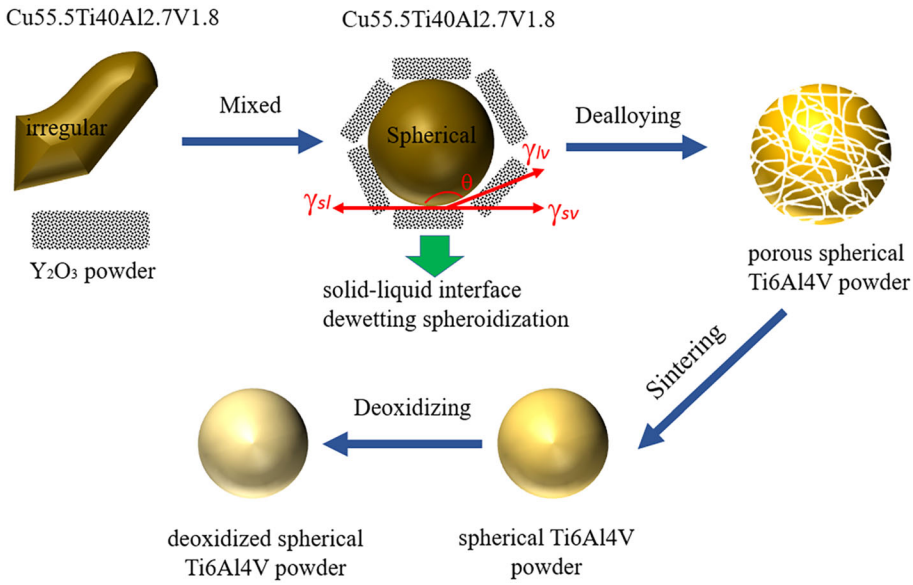

Fig. 1. Schematic diagram of the preparation processes.

state dispersed by the solid dispersant formed spheres with a better degree of sphericity. Once the process is complete, the target spherical metal powder could be obtained by cooling and removing the dispersant.[24] In this method, the selection of a suitable solid dispersant and controlling the environment and temperature during the spheroidization process are important factors in achieving optimal results. It is crucial is to prevent any significant diffusion reaction between the metal droplets and the solid dispersant at high temperatures, as this can reduce the surface energy of the solid/liquid interface and introduce impurities, resulting a poor spheroidization effect. However, the Ti6Al4V alloy poses challenges due to its high melting point, toughness, and high temperature activity. When the solid–liquid interface dewetting spheroidization method was used to prepare spherical Ti6Al4V powder, problems of high spheroidizing temperature, easy oxidation, and difficulty in finding suitable solid dispersants would be encountered.[27]

In previous studies, by taking the intermetallic compound pre-alloys of TiCu and $TiAlCu_2$, we successfully prepared spherical powders of Ti and TiAl alloys though the copper-assisted spheroidization method.[28,29] However, the pre-alloys of binary or ternary intermetallic compounds with a stable and determined structure could not be applied to the more wildly used Ti6Al4V alloy because of the multicomponent and dual-phase nature of α and β. According to the phase diagram, the Ti-Cu system offers several kinds of intermetallic compounds such as TiCu, Ti_2Cu, Ti_3Cu_4, Ti_2Cu_3, $TiCu_2$, and $TiCu_4$. Among them, the calculated results reveal that the TiCu alloy with an atomic ratio about 1:1 has a low melting point of 982°C and exhibits the most negative formation enthalpy (ΔE_f), indicating the strongest bonds and a better stability.[30] Therefore, we tried to introduce copper element and designed a pre-alloy of Cu40Ti2.7Al1.8V intermetallic compound with a composition close to TiCu to conduct the solid-liquid interface dewetting spheroidization process and prepared the spherical Ti6Al4V powder by copper-assisted spheroidization method. The melting point of Ti-Cu alloy, which is close to the composition of Cu40Ti2.7Al1.8V, is < 1000°C, making it much simpler to spheroidize compared to Ti6Al4V alloy (with a melting point of about 1600°C). Additionally, as an intermetallic compound, the Cu40Ti2.7Al1.8V alloy is easy to break mechanically, allowing us to obtain suitably sized Cu40Ti2.7Al1.8V particles through simple sieving.[30,31] Therefore, it is possible to find a suitable solid dispersant powder and prepare spherical Cu40Ti2.7Al1.8V powder with a controllable particle size when using the solid-liquid interface dewetting spheroidization method. Y_2O_3, an oxide ceramic material with a high melting point (> 2400°C) and strong high-temperature stability, is commonly used to produce shell mold materials for casting titanium alloys.[32,33] Y, as a rare earth element, can be used to prepare titanium alloys by reduction at high temperature,[34,35] which indicates the low oxygen diffusion between Y_2O_3 and titanium alloys. Therefore, in this study, Y_2O_3 powder was used as the candidate solid dispersant powder to prepare the spherical Cu40Ti2.7Al1.8V powder.

Figure 2a shows the Cu40Ti2.7Al1.8V pre-alloy particles after manual grinding and sieving, which exhibit an irregular shape. The SEM images of the Cu40Ti2.7Al1.8V pre-alloy particles prepared by the solid–liquid interface dewetting spheroidization method are shown in Fig. 2b and c. The morphologies of the Cu40Ti2.7Al1.8V pre-alloy particles show a relatively uniform size distribution and good

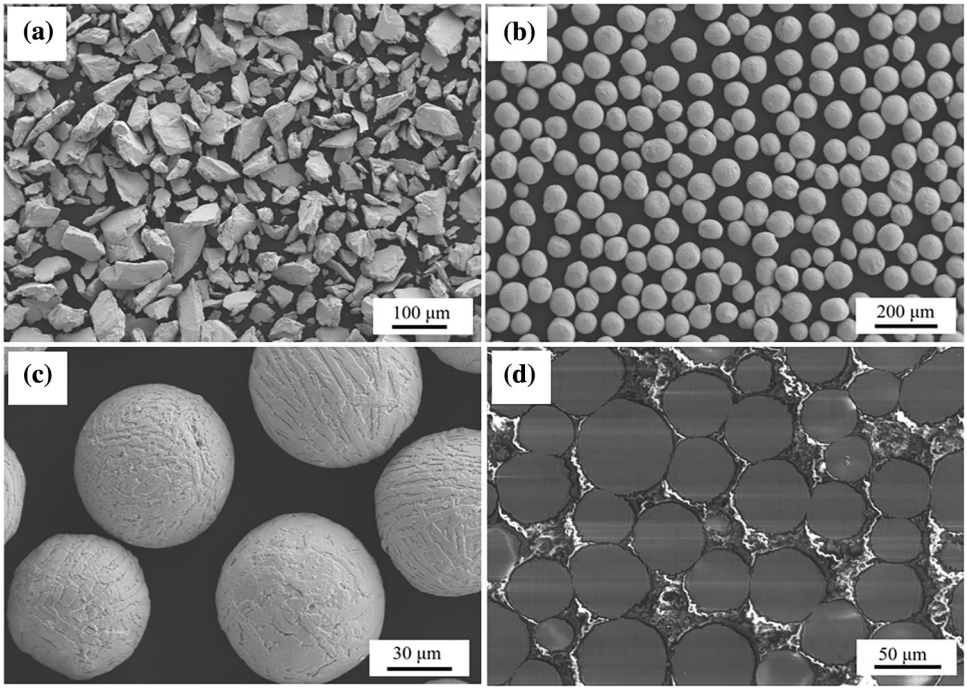

Fig. 2. SEM images of: (a) irregular Cu40Ti2.7Al1.8V powder; (b, c) Cu40Ti2.7Al1.8V powder after spheroidization; (d) cross-sectional morphology of the spherical Cu40Ti2.7Al1.8V powder.

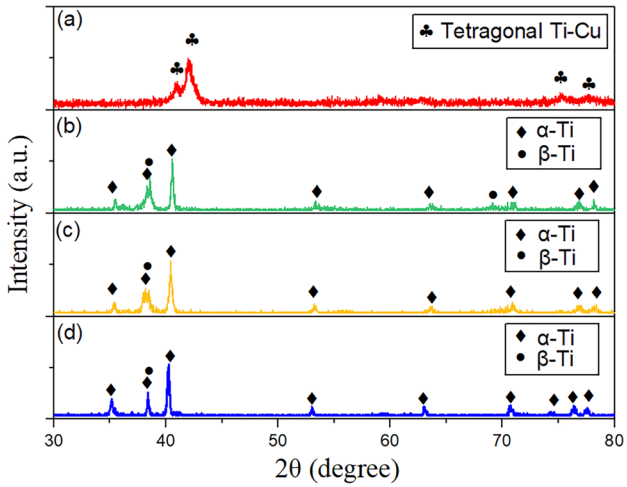

Fig. 3. X-ray diffractograms of the powders: (a) Cu40Ti2.7Al1.8V pre-alloy particles after spheroidization; (b) porous Ti6Al4V powder after dealloying and water washing; (c) sintered Ti6Al4V sphere; (d) final deoxidized Ti6Al4V sphere.

sphericity. As shown in Fig. 2d, the cross section of the spherical Cu40Ti2.7Al1.8V particles shows a dense morphology, and there is no hollow powder similar to that caused during the atomization process. The XRD patterns of the spherical Cu40Ti2.7Al1.8V particles are shown in Fig. 3a. After the spheroidization process, the particles show a tetragonal structure Ti-Cu phase with broadened peaks, consistent with that of Ti-Cu phase in the phase diagram.[30]

Preparation of Spherical Porous Ti6Al4V Powder

To obtain the spherical Ti6Al4V powder, the Cu element was initially removed from the Cu40Ti2.7Al1.8V pre-alloy powder. Liquid metal dealloying (LMD) is a novel technique for preparing porous materials by removing specific elements in the precursor materials based on the differences of the mixing enthalpy between the materials. Due to the strong reducibility of the metal melts, this method can avoid the oxidation phenomenon of the sample. Furthermore, by adjusting the reaction time, temperature, and other conditions, the morphology and other characteristics of the final porous materials could be controlled, making them a hotspot in the preparation of porous titanium alloys.[36] As demonstrated in Fig. 4a, taking Ti-Cu alloy as an example, most of the current LMD studies are carried out by immersing the precursor Ti-Cu alloy in liquid Mg. Usually the Ti-Cu alloy shows a morphology of bulk or flake, and dealloying process can proceed smoothly.[37,38] However, as demonstrated in Fig. 4b, when dealing with micron-sized Ti-Cu alloy particles, due to the surface tension and the stickiness of the liquid Mg, there are voids between the Ti-Cu particles when directly immersed in the melt, resulting the uneven contact between liquid Mg and Ti-Cu particles. Then, the poor dealloying effect occurs. To address this, a simpler and more feasible dealloying process was applied in this work. As shown in Fig. 4c, the Mg-$MgCl_2$ powder was used as the melt for dealloying

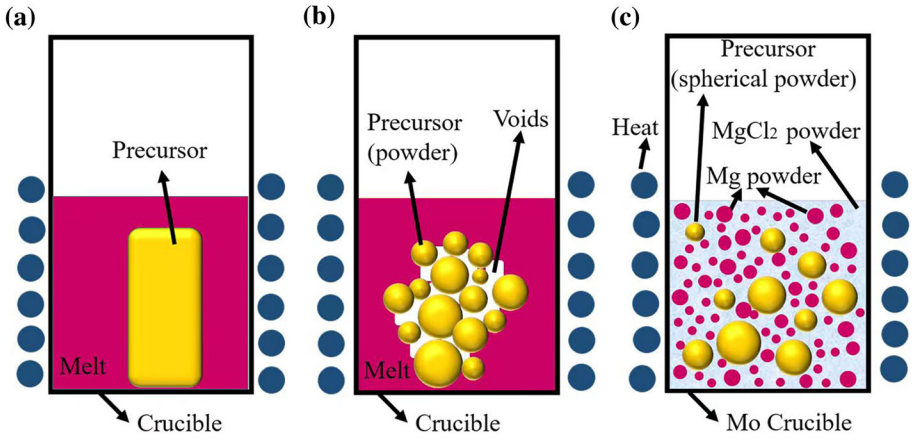

Fig. 4. Schematic diagram of the dealloying process with precursors possessing different morphologies: (a) flaky or blocky precursor immersed in liquid melt; (b) micron-sized granular precursor immersed in liquid melt; (c) micron-sized granular precursor mixed with $MgCl_2$-Mg powder in this work.

process. The process involved mixing the spherical Cu40Ti2.7Al1.8V powder and Mg-$MgCl_2$ powder evenly and placing them in a Mo crucible to carry out the dealloying process at 845°C. The even mixing facilitated uniform contact between the Mg particles and the spherical Cu40Ti2.7Al1.8V alloy particles. Simultaneously, when the temperature exceeded the melting point, Mg partially dissolved in liquid $MgCl_2$[39] and uniformly wrapped around the spherical Cu40Ti2.7Al1.8V powder, thereby enhancing the uniformity of dealloying. Therefore, the disadvantages encountered by using pure Mg melts as the dealloying medium could be avoided.

Figure 5 displays the cross-sectional element distribution of the particles after the dealloying process and water washing. It is evident that the distribution areas of Cu and Mg elements are consistent and segregated from the distribution areas of Ti and V elements. Usually, the following Eq. 2 is used to describe the liquid metal dealloying progress of the precursor alloy and dealloying melt:[36]

$$\Delta G_{\text{mix}} = \Delta H_{\text{mix}} - T\Delta S_{\text{mix}} \quad (2)$$

where the T is the absolute temperature, ΔG_{mix} means the free energy of mixing, and ΔH_{mix} and ΔS_{mix} are the heat and entropy of mixing, respectively. If the $\Delta H_{\text{mix}} < 0$, the ΔG_{mix} is negative at a certain temperature, the dealloying progress occurs spontaneously. In the studied Ti-Al-V-Cu and Mg system, the ΔH_{mix} values of Ti-Mg and V-Mg are positive, while that of Cu-Mg is negative. In the dealloying process, the Cu element in the spherical Cu40Ti2.7Al1.8V powder was dissolved in the liquid Mg, while Ti and V elements were insoluble in Mg melt, resulting in a reticular and porous alloy made of Ti and V elements.[37,38] Notably, the ΔH_{mix} value of Al-Mg is negative, indicating that the Al element is prone to loss. However, the element-enriched areas of Al element are consistent with Ti and V, as shown in Fig. 5a4, a5, and a6. Additionally, Table I presents the particle composition post dealloying and acid leaching processes. The elemental content of Mg and Cu is significantly low, while the elemental contents of Al and V are 5.94 wt.% and 3.916 wt.%, respectively. These values are consistent with the ratio of Ti, Al, and V elements in the configured Cu40Ti2.7Al1.8V pre-alloy, with nearly no loss of Al. Al-Mg and Al-Ti are both negative mixed enthalpy alloy systems,[40] and we believe that in the studied dealloying temperature range, Al and Ti may form more stable solid solutions or intermetallic compounds than Al and Mg. It is reported that TiAl and Ti_3Al are more stable than Al_2Mg_3 or $Al_{12}Mg_{17}$ at 300–1000°C, and the Ti6Al4V alloy or Ti-48Al-2Cr-2Nb alloy powder can be prepared by co-reducing Ti, Al, and V oxides or Ti, Al, Cr, and Nb oxides with molten Mg or Mg-Ca.[41,42] Our research results also confirm that during the process of molten Mg-$MgCl_2$ dealloying, Al in Cu40Ti2.7Al1.8V alloy will not react with Mg but forms Ti-Al-V alloy with Ti and V.

Figure 6 shows the SEM images of the spherical porous Ti6Al4V particles obtained after dealloying and acid leaching cleaning process. Figure 6a and b shows that the cleaned porous Ti6Al4V particles exhibit a spherical porous structure, and they are consistent with the morphology of the spherical Cu40Ti2.7Al1.8V powder. Figure 6c and d indicates the cross-sectional view of the spherical porous Ti6Al4V particles, which shows a uniform dealloying effect, and the average width of the porous Ti6Al4V particles is about 5.24 μm ± 0.7 μm. Depending on the characteristics of the LMD, the toughness and porosity of the spherical porous Ti6Al4V particles could be controlled by adjusting the temperature and time of corrosion. The XRD pattern of the porous sphere is shown in Fig. 3b, revealing a structure of the main phase of α and a

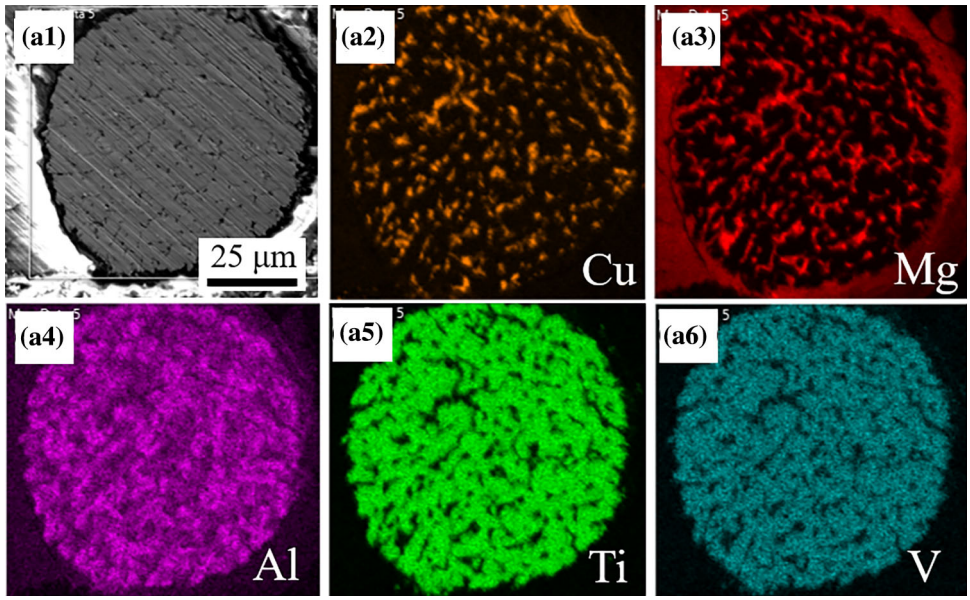

Fig. 5. Cross-sectional element distribution of the particles after dealloying process and water washing: (a1) cross-section; (a2–a6) element distribution of Cu, Mg, Al, Ti, V, respectively.

Table I. Element composition of the Ti6Al4V powder after each step

Element (wt.%)	Al	V	Cu	Mg	Y	Ti
Dealloyed	6.23	3.72	0.271	0.244	< 0.009	Bal.
Sintered	5.7	3.58	0.23	< 0.005	< 0.009	Bal.
Deoxidized	5.94	3.916	< 0.005	< 0.005	< 0.009	Bal.

small amount of β phase, consistent with two-phase structure of Ti6Al4V.[2,3]

Sintering and Deoxidizing

To prevent the bonding effect between Ti6Al4V alloy particles during high-temperature sintering treatment, Y_2O_3 powder was utilized to disperse the spherical porous Ti6Al4V alloy particles. The XRD pattern of the sintered Ti6Al4V particles in Fig. 3c shows that the Ti6Al4V alloy structure of the main phase of α and a small amount of β phase is still maintained. Figure 7a and b shows the morphologies of the Ti6Al4V particles after sintering. The particles still maintain a good sphericity without any phenomenon of mutual adhesion. However, the surface of the particles is relatively rough because of the small amount of oxygen diffusion between the particles and Y_2O_3 during sintering treatment. The cross-sectional view in Fig. 7c shows that the sintered particles are dense and free of voids inside. In our work, a eutectic salt deoxygenation method similar to the GSD method was adopted.[16] The morphologies of the particles after deoxidation treatment are shown in Fig. 7d and e. After deoxidation, the particles still keep the overall morphology of the sintered Ti6Al4V particles, and the roughness of the surface is greatly reduced. The smoother surface of powder after deoxygenation treatment is conducive to improving the powder fluidity and packing density, and the powder with lower surface roughness and smoother surface is also the ideal PBF-AM feedstock. Moreover, the spherical powders with suitable surface roughness would facilitate the laser absorption behavior during the printing process.[43,44] After the deoxidation process, the oxygen content of the final reduction particles was reduced from 2195.7 ppm of the sintered particles to 250 ppm. It is reported that the spherical powder with low oxygen content has many advantages in AM, e.g., in the research on the AM process of 304L stainless steel, the powder with low oxygen content is conducive to improving the ductility of the manufactured parts.[45] The XRD pattern of the deoxidized Ti6Al4V particles is shown in Fig. 3d, the Ti6Al4V powder possesses a main phase of α, and the small amount of β phase is weaker and nearly undetectable. The particle size distribution of the Ti6Al4V particles after deoxidation is shown in Fig. 7f. The particles are distributed in the range of 30–100 μm as a whole. This broad

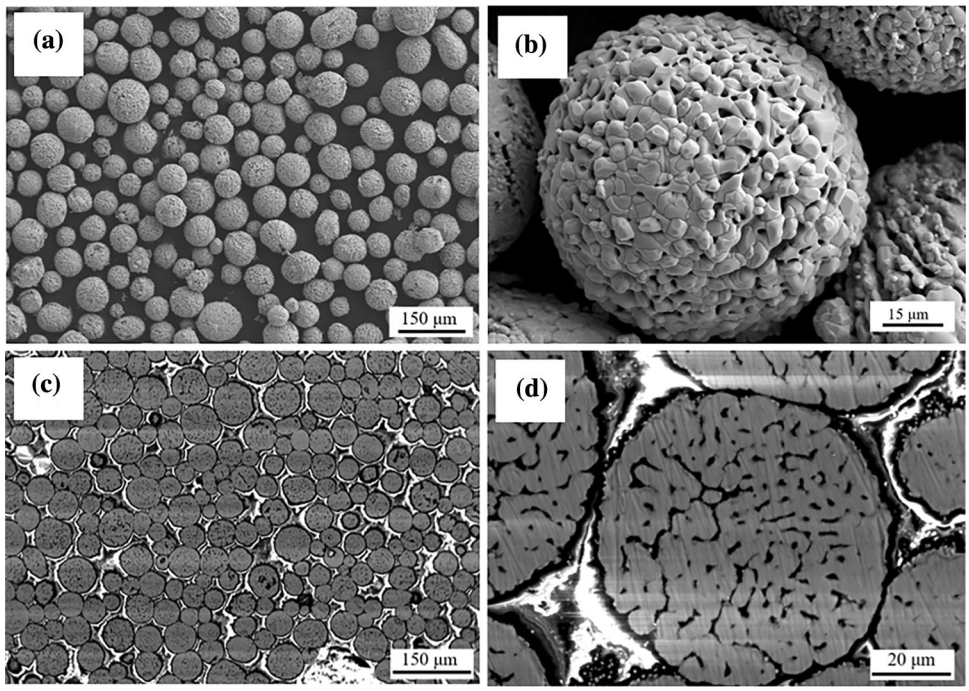

Fig. 6. Large-scale and enlarged SEM images of the porous Ti6Al4V spheres: (a, b) surface; (c, d) cross-section.

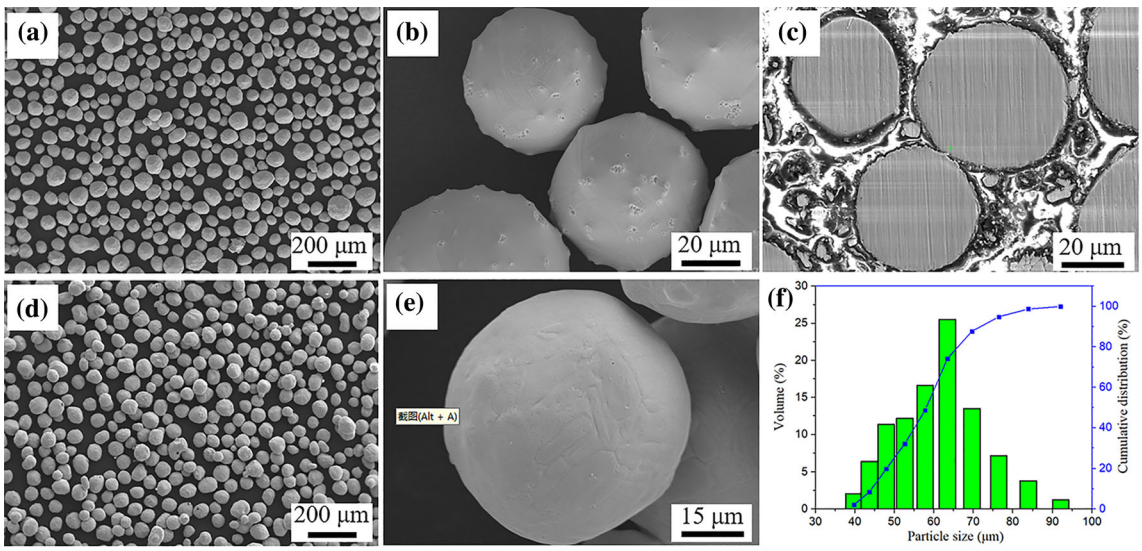

Fig. 7. SEM micrographs of: (a, b) the sintered Ti6Al4V powder and (c) its cross section; (d, e) the deoxidized Ti6Al4V powder and (f) the particle size distribution of the deoxidized Ti6Al4V powder.

particle size distribution is also an ideal characteristic of PBF-AM feedstock.[44] Notably, the final particle inherited several morphological characteristics of the spherical Cu40Ti2.7Al1.8V particles, where the size of the spherical Ti6Al4V particles is determined by the particle size of Cu40Ti2.7Al1.8V particles. Therefore, this method can improve the yield of Ti6Al4V spheres with target size distribution by mechanical grinding and sieving of Cu40Ti2.7Al1.8V particles with appropriate particle size.

CONCLUSION

In conclusion, a novel copper-assisted spheroidization method for preparing spherical Ti6Al4V particles was developed in this study. The morphology, structure, and composition of the sample during each preparation process were investigated. The spherical Ti6Al4V particles prepared by the method possess the characteristics of low oxygen content, good sphericity, and controllable particle size distribution and may potentially meet the

requirements of additive manufacturing. Furthermore, this method offers a promising approach for preparing various spherical porous alloy powders and spherical alloy powders with a high melting point.

ACKNOWLEDGEMENTS

This work was supported by the National Natural Science Foundation of China (No. 51671102).

DATA AVAILABILITY

Data will be made available on request.

CONFLICT OF INTEREST

The authors declare that they have no known competing financial interests or personal relationships that could have appeared to influence the work reported in this paper.

ETHICAL APPROVAL

Authors state that the research was conducted according to ethical standards.

REFERENCES

1. R.R. Boyer, *Mater. Sci. Eng. A* 213, 103 (1996).
2. C. Leyens and M. Peters, *Titanium and Titanium Alloys: Fundamentals and Applications*, 1st edn. (Wiley, Weinheim, 2003), pp1–36.
3. G. Lütjering and J.C. Williams, *Titanium*, 2nd edn. (Springer Press, Berlin, 2007), pp15–52.
4. A.R. McAndrewk, P.A. Colegrove, C. Bühr, B.C.D. Flipo, and A. Vairis, *Prog. Mater. Sci.* 92, 225 (2018).
5. L.C. Zhang and H. Attar, *Adv. Eng. Mater.* 18, 463 (2016).
6. J. Dawes, R. Bowerman, and R. Trepleton, *Johns. Matthey Technol.* 59, 243 (2016).
7. M. Attaran, *Bus. Horiz.* 60, 677 (2017).
8. B. Berman, *Bus. Horiz.* 55, 155 (2012).
9. Q. Ma, *Mater. China* 30, 50 (2011).
10. F.H. Froes and B. Dutta, *Adv. Mater. Res.* 1019, 19 (2014).
11. C. Chua, S.L. Sing, and C.K. Chua, *Virtual Phys. Prototyp.* 18, e2138463 (2022).
12. C.Y. Lu, X.D. Jia, J. Lee, and J. Shi, *Virtual Phys. Prototyp.* 17, 787 (2022).
13. D.N. Luu, W. Zhou, and S.M.L. Nai, *Mater. Sci. Addit. Manuf.* 1, 25 (2022).
14. J. Gardan, *Int. J. Prod. Res.* 54, 3118 (2016).
15. M. Boulos, *Nucl. Eng. Technol.* 44, 1 (2012).
16. P. Sun, Z.Z. Fang, Y. Xia, Y. Zhang, and C.S. Zhou, *Powder Technol.* 301, 331 (2016).
17. W. Xu, S.Q. Xiao, G. Chen, C.C. Liu, and X. Qu, *J. Mater. Sci. Technol.* 35, 322 (2019).
18. C.F. Yolton and F.H.S. Froes, *Titanium Powder Metall.* 2, 21 (2015).
19. G. Wegmann, R. Gerling, and F.P. Schimansky, *Acta Mater.* 51, 741 (2003).
20. G. Chen, S.Y. Zhao, P. Tan, J. Wang, C.S. Xiang, and H.P. Tang, *Powder Technol.* 333, 38 (2018).
21. G. Chen, Q. Zhou, S.Y. Zhao, J.O. Yin, P. Tan, Z.F. Li, Y. Ge, J. Wang, and H.P. Tang, *Powder Technol.* 330, 425 (2018).
22. N.A. Yefimov, *Handbook of Non-ferrous Metal Powders: Technologies and Applications*, 1st edn. (Elsevier Press, Burlington, 2009), pp125–185.
23. J.J. Tang, Y. Nie, Q. Lei, and Y.P. Li, *Adv. Powder Technol.* 30, 2330 (2019).
24. Z.Z. Cheng, C.L. Lei, H.F. Huang, S.L. Tang, and Y.W. Du, *Mater. Des.* 97, 324 (2016).
25. C.L. Lei, H.F. Huang, Z.Z. Cheng, S.L. Tang, and Y.W. Du, *Appl. Surf. Sci.* 357, 167 (2015).
26. Y. Huang, J. Qian, D.S. Dong, Y.G. Shi, Y.W. Du, and S.L. Tang, *J. Magn. Magn. Mater.* 543, 168621 (2022).
27. X.J. Liao, Q. Lai, and S.L. Zhang, *Iron Steel Vanadium Titan.* 05, 1 (2017).
28. J. Qian, D.S. Dong, G. Wei, M. Shi, and S.L. Tang, *Powder Technol.* 411, 117927 (2022).
29. J. Qian, B. Yin, D.S. Dong, G. Wei, M. Shi, and S.L. Tang, *J. Mater. Res. Technol.* 25, 1860 (2023).
30. L. Arijit, K. Bhanumurthy, G. Kale, and B. Kashyap, *Int. J. Mater. Res.* 103, 661 (2012).
31. S.Y. Liu and Y.C. Shin, *Mater. Des.* 164, 107552 (2019).
32. F. Gomes, H. Puga, J. Barbosa, and C.S. Ribeiro, *J. Mater. Sci.* 46, 4922 (2011).
33. Y.M. Wei, Z.G. Lu, X.Y. Li, and X. Guo, *Rare Met.* 38, 327 (2019).
34. K.T. Jacob and S. Gupta, *JOM* 61, 56 (2009).
35. T. Tanaka, T. Ouchi, and T.H. Okabe, *Mater. Trans.* 61, 1967 (2020).
36. X.Y. Guo, C.X. Zhang, Q.H. Tian, and D.W. Yu, *Mater. Today Commun.* 26, 102007 (2021).
37. M. Tsuda, T. Wada, and H. Kato, *J. Appl. Phys.* 114, 113503 (2013).
38. I.V. Okulov, A.V. Okulov, A.S. Volegov, and J. Markmann, *Scr. Mater.* 154, 68 (2018).
39. Y. Zhang, Z.Z. Fang, P. Sun, Y. Xia, M. Free, Z. Huang, H. Lefler, T.Y. Zhang, and J. Guo, *Chem. Eng. J.* 327, 169 (2017).
40. A. Takeuchi and A. Inoue, *Mater. Trans.* 46, 2817 (2005).
41. X.Y. Guo, Z.W. Dong, Y. Xia, P.D. Liu, H.N. Liu, Q.H. Tian, and T. Nonferr, *Met. Soc.* 32, 1351 (2022).
42. J.S. Yan, Z.H. Dou, and L.P. Niu, *Rare Met. Mater. Eng.* 50, 2973 (2021).
43. J.J. Sun, M. Guo, K.Y. Shi, and D.D. Gu, *Mater. Sci. Addit. Manuf.* 1, 11 (2022).
44. S. Yim, H. Bian, K. Aoyagi, K. Yamanaka, and A. Chiba, *Addit. Manuf.* 49, 102489 (2022).
45. M. Sehhat, A. Sutton, C. Hung, B. Brown, R. O'Malley, J.K. Park, and M. Leu, *Mater. Sci. Addit. Manuf.* 1, 1 (2022).